Multilayered pore-closed PLGA microsphere delivering OGP and BMP-2 in sequential release patterns for the facilitation of BMSCs osteogenic differentiation

Bing-jun Zhang,[1] Zhi-wei Han,[1] Ke Duan,[1] Yan-dong Mu,[2] Jie Weng[1]

[1]Key Laboratory of Advanced Technologies of Materials (Ministry of Education), School of Materials Science and Engineering, Southwest Jiaotong University, Chengdu, Sichuan 610031, People's Republic of China
[2]Dental Department, Sichuan Province People's Hospital, Chengdu, Sichuan 610072, People's Republic of China

Abstract: Bone tissue regeneration may be more effectively administrated by controlled release of multiple biofactors, given that bone healing comprises a cascade of biological events controlled by numerous cytokines and growth factors (GFs). Here, we propose a novel microcarrier with the capability to sequentially deliver dual biofactors for better controlling the bone regeneration process. First, osteogenic growth peptide (OGP) was incorporated in porous poly(lactic-*co*-glycolic) acid (PLGA) microspheres by a simple solution dipping method and subsequent pore-closing treatment. Then, a multilayered polyelectrolyte coating ((HA-CS)$_2$-Hep-BMP-2-Hep-(CS-HA)$_2$) was prepared on the surface of such OGP-loaded pore-closed PLGA microspheres by layer-by-layer assembly. Results showed that the OGP release was minimal ($<$17.1%) in the first 15 days but accelerated remarkably thereafter, while at least 60.3% of the bone morphogenetic protein-2 (BMP-2) load was released in the first 15 days and only very slow release was observed subsequently. Further *in vitro* cell experiments showed that the dual-biomolecule-loaded microspheres elicited more cells with extremely elongated cellular morphology, much higher alkaline phosphatase level and upregulated expression of osteocalcin. Such a dual loading of OGP and BMP-2 had a more positive impact on bone marrow mesenchymal stem cells proliferation and osteogenic differentiation compared with either OGP or BMP-2 alone, suggesting potential synergistic benefit of the sequential release of multiple peptide-based biofactors in a coordinated manner. Overall, this dual delivery system may provide a therapeutic strategy sequentially targeting multiple events (or mechanisms) during bone healing, which is believed to benefit the regenerative repair of bone defects. © 2017 Wiley Periodicals, Inc. J Biomed Mater Res Part A: 106A: 95–105, 2018.

Key Words: dual loading, OGP, BMP-2, sequential release, osteogenic differentiation

---

INTRODUCTION

Bone healing comprises a cascade of biological events (e.g., inflammatory response, angiogenesis, and osteogenesis) controlled by numerous cytokines and growth factors (GFs). These biofactors are sequentially and differentially expressed at the site of injury to coordinately control the activities of cells involved, such as differentiation, proliferation, and matrix production.[1–5]

Currently, two categories of biofactors are known to stimulate the osteogenic activities of cells. The first category induces the transformation of nonosteoblastic cells to osteoblasts. This effect is known as induction, and these factors are classified as inductors. The second category increases the proliferation or osteoblastic activity of osteoblasts, thus accelerating ossification and bone matrix formation. These effects are classified as modulation. Induction and modulation both play critical roles during bone healing, although their relative importance may vary during different stages of the process. In fact, the two categories of biofactors do not exert function in isolation in an effective way but, instead, work synergistically.[6]

Many studies on biomaterial-assisted bone repair have used induction or modulation, but most of these have been confined to the study of the effect of one biofactor. More recently, inspired by the physiology of bone healing, Raiche et al. reported that, compared with single delivery of Co ions incorporated into an alginate-based shell or bone morphogenetic protein-2 (BMP-2) loaded in a collagen-based core from core–shell fibrous hydrogel, sequential release of the two factors significantly enhanced bone formation.[7]
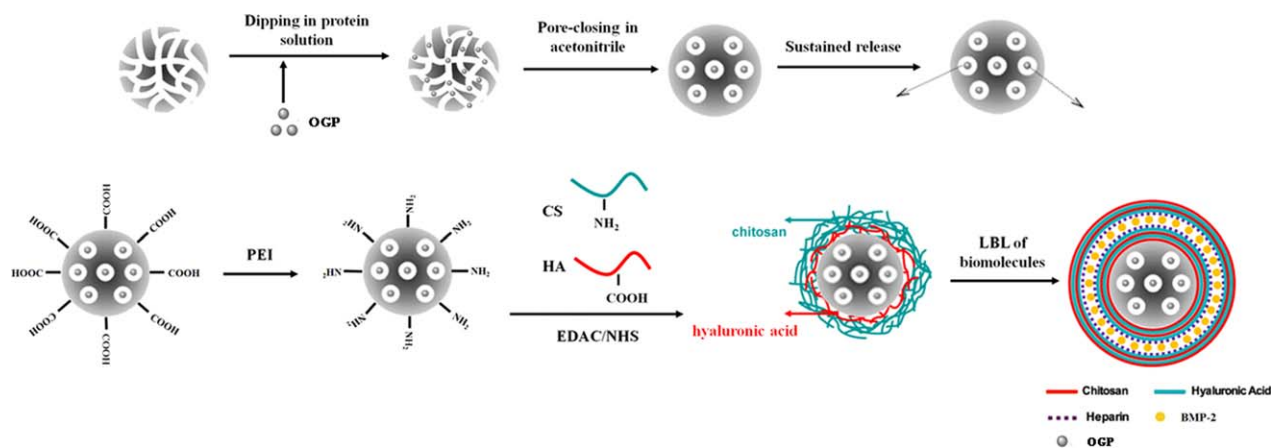
FIGURE 1. Illustration of procedures for peptide drug delivery by a multilayered structure on the surface of PLGA microspheres.

Various delivery vehicles have been developed to regulate the release behaviors of biofactors. Of these, poly(lactic-*co*-glycolic acid) (PLGA) microspheres, commonly prepared by a water-in-oil-in-water double-emulsion method, were promising candidates because of their safety, biodegradability, and successful application in clinics.[8] However, the shear stress and the presence of an aqueous/organic interface during emulsion preparation may adversely affect the structural integrity of biofactors (e.g., proteins) and cause their denaturation and aggregation.[9,10] Therefore, porous PLGA microspheres have been proposed as an alternative carrier for the release of protein biofactors. In this design, factors are entrapped in the pores of microspheres by solution soaking, thus protecting their bioactivities. However, current porous microspheres frequently fail to offer a satisfactory controlled release behavior. Sun et al.[11] and Lee et al.[12] found that, porous PLGA microspheres carrying human serum albumin and insulin released 88.7% and 50% of the two biofactors within 1 day, respectively. Furthermore, although some studies have explored the codelivery of multiple biofactors, in most cases different biofactors were released simultaneously instead of sequentially.[13–17] Sequential release of multiple biofactors from one carrier, which is technically more difficult, is thought to offer important advantages, because different signals may be required at different stages of bone healing. Therefore, it is necessary to develop porous PLGA microspheres allowing effective sequential release of multiple osteogenic biofactors.

The present study reports a novel approach to achieve the sequential release of two osteogenic biofactors (osteogenic growth peptide [OGP] and recombinant human BMP-2) from porous PLGA microspheres. We will also demonstrate that this sequential release produced synergistically positive effects on *in vitro* osteogenic differentiation of bone-marrow-derived stem cells.

MATERIALS AND METHODS
Preparation of OGP-loaded porous PLGA microspheres
PLGA (200 mg; lactide:glycolide = 50:50, Mw = 30 kDa; Daigang Biotech, Jinan, Shandong, China) was dissolved in 4 mL of CH_2Cl_2. NH_4HCO_3 (5 mg) was dissolved in 1.5 mL of deionized water to form the inner aqueous phase (W_1). Subsequently, W_1 was added to the PLGA/CH_2Cl_2 solution and homogenized (6000 rpm, 60 s; FSH-2A, Anpu Instruments Ltd., Nanjing, Jiangsu, China) to form the primary emulsion (W_1/O). The emulsion was dropped into 50 mL of a 0.5% (w/v) aqueous poly(vinyl alcohol) (PVA, 99% hydrolysis, 85 kDa) solution (outer aqueous phase; W_2) and stirred (500 rpm) to give a double emulsion (W_1/O/W_2). Then, the CH_2Cl_2 in the oil phase was evaporated off by stirring for 4 h. The microspheres were collected by centrifugation (3000 rpm, 3 min), rinsed thrice with deionized water, and lyophilized (Biosafer-10A, Biosafer, Hong Kong, China). OGP (11.5 kDa; Xinjingke Biotech, Beijing, China) was loaded in PLGA microspheres by dispersing these microspheres (1.0 g) in 10 mL of an OGP solution (0.1 mg/mL, in 10 mM phosphate buffer, pH 7.4) and gently shaking (37°C, 24 h). OGP-loaded microspheres were recovered by centrifugation. Unless otherwise stated, all chemicals were reagent grade and purchased from Kelong Chemical (Chengdu, Sichuan, China).

Pore-closing treatment of OGP-loaded microspheres
OGP-loaded PLGA microspheres (100 mg) were dispersed in 2 mL of water, and acetonitrile (AN) was added to the suspension under stirring at a series of concentrations (0–10%, v/v), as a water miscible solvent. After interaction for 15 min, this pore-closing treatment (Fig. 1, upper row) was terminated by adding 20 mL of water, and the microspheres were recovered.

Layer-by-layer coating of polyelectrolyte multilayers on microspheres
PEI immobilization of microsphere surface. To retard factor release from the microspheres, they were layer-by-layer coated with polyelectrolyte multilayers as follows. First, OGP-loaded pore-closed PLGA microspheres were treated in 10 mL of a pH 5.5 buffer (0.1 M 2-morpholinoethanesulfonic acid [MES], Xinjingke Biotech) with 95.9 mg of 1-ethyl-3-(3-dimethyl-aminopropyl)-carbodiimide hydrochloride (EDC), and 57.6 mg of N-hydroxysuccinimide (NHS, both from Bomeibio, Hefei, China) for 5 min to activate the

uncapped free carboxylic groups in the terminal ends of the PLGA chains (Fig. 1, lower row), and recovered by centrifugation. Then PLGA microspheres were aminolyzed by immersing in a 50 mg/mL polyethylenimine (PEI) solution (600 Da, Sigma) for 10 min under stirring. PEI-immobilized OGP-loaded PLGA microspheres were labeled[18] with fluorescein isothiocyanate (FITC, Sigma). The FITC-labeled microspheres were studied by laser scanning confocal microscopy (LSM510, Carl Zeiss, Jena, Germany).

Layer-by-layer coating and BMP-2 adsorption. Three kinds of polyelectrolyte solutions were prepared: 10 mg/mL chitosan (CS, viscosity: 286 cps) in 0.1 M acetic acid (i.e., stock solution), 0.2 mg/mL CS in 10 mM MES buffer, 0.2 mg/mL hyaluronic acid (HA) in 10 mM MES buffer, and 0.2 mg/mL heparin (Hep, all from Bomeibio) in 10 mM MES buffer. A dimethylformamide (DMF) solution containing 50 mg/mL EDC and 100 mg/mL NHS was prepared shortly before use. The DMF solution was separately added to the above HA and Hep solutions at 1% (v/v), and allowed to crosslink these molecules for 10 min before incubation with the aminolyzed PLGA microsphere surfaces.

For polyelectrolyte multilayer coating (Fig. 1, lower row), PEI-immobilized microspheres (10 mg) were suspended in 1 mL of a polyelectrolyte (e.g., CS, Hep, or HA) solution and gently shaken at 37°C for 15 min to ensure maximal binding. Then, they were recovered by centrifugation, rinsed twice with 1 mL of the MES buffer, and immersed in another polyelectrolyte solution for binding of the next layer. For BMP-2 adsorption, the microspheres were incubated in a 7.5 µg/mL recombinant human BMP-2 (26 kDa; Xinjingke Biotech) solution in PBS for 15 min to allow effective binding to the underlying layer (Fig. 1, lower row).

By these procedures, BMP-2 and polyelectrolytes were deposited on the OGP-loaded microspheres in the sequence: (HA-CS)$_2$-Hep-BMP-2-Hep-(CS-HA)$_2$ (Fig. 1), denoted as PMs (OGP/BMP-2). As previously reported,[19] the deposition of 5.5 bilayers were selected to ensure the formation of more uniform coating on the PLGA microspheres and reduce BMP-2 leakage for subsequent a significantly lower release rate constants. Hep was added to facilitate the binding of BMP-2 to the polyelectrolyte layers and maintain its bioactivity.[20] Factor-free microspheres and those carrying OGP alone or those carrying BMP-2 alone were also prepared through the same treatment and noted as PMs, PMs (OGP), and PMs (BMP-2).

Characterization of LbL-coated microspheres

Surface morphology of microspheres was studied by scanning electron microscopy (SEM; JEOL JSM 6480LV). Mean diameters of microspheres and pores on their surfaces were measured by image analyses of 50 SEM micrographs. Functional groups on PEI-immobilized and LbL-coated PLGA microspheres were characterized by Fourier-transform infrared (FTIR) spectroscopy (Nicolet 5700). To characterize the changes of microsphere properties with increasing polyelectrolyte layers, samples of CS were labeled with either Rhodamine-B or FITC following manufacturer instructions (Supporting Information Fig. S1). PLGA microspheres were coated with 11 layers of polyelectrolytes as described above in previous section, except that the second layer used was Rhodamine-B-labeled CS and the eighth layer was FITC-labeled CS. The sample of LbL-coated PLGA microspheres was analyzed by confocal laser scanning microscopy. Then, the Zeta potentials of microspheres were also measured (Zetersizer Nano Z; Malvern Instruments, Malvern, UK).

In vitro release

LbL-coated microspheres (20 mg) were suspended in 1.5 mL of PBS supplemented with 0.01% (w/v) sodium azide and 0.02% (w/v) Tween 20, and placed in a rotary incubator (37°C) for 60 days. The media was periodically sampled (0.5 mL) for analysis and replenished. OGP and BMP-2 concentrations in the samples were analyzed with enzyme-linked immunosorbent assay (ELISA) kits (Ray Biotech, Norcross, GA). The amount of BMP-2 immobilized onto the multilayered pore-closed PLGA microspheres or the amount of OGP loaded onto the porous microspheres was calculated from the difference in BMP-2 or OGP concentration in the loading solution before and after BMP-2 or OGP loading via ELISA. Afterwards, PMs(BMP-2) and PMs(BMP-2/OGP) were exposed to 1 mL of 0.5 N NaOH solution, respectively. After the microspheres were completely hydrolyzed, the solution was neutralized and the incorporated protein content was analyzed by using a BCA protein assay kit. Thus, the encapsulated OGP amount in the microspheres was calculated by subtracting the BMP-2 amount in PMs(BMP-2) from the total protein amount in PMs(BMP-2/OGP). Subsequently, the cumulative release profile was calculated. The BMP-2 or OGP encapsulation efficiency (E_{encaps}) was given as $E_{encaps}(\%) = M_{encaps}/M_{feed} \times 100\%$, in which the M_{encaps} was the amount of encapsulated BMP-2 or OGP, and M_{feed} was the total feed amount of BMP-2 (BMP-2/microspheres, 7.5 µg/10 mg, w/w) or OGP (OGP/microspheres, 1 mg/1 g, w/w), as described in the preparation method.

Bioactivity characterizations

Primary rat bone marrow mesenchymal stem cells (BMSCs) were isolated and expanded on the basis of protocols previously described.[21] Briefly, the bone marrow was obtained from Sprague–Dawley rats (age: 1 week; Dashuo Biotech, Chengdu, China) by cutting off both ends of the femora. Cells were cultured in Dulbecco's modified Eagle medium (DMEM; Hyclone, USA) containing 10% fetal bovine serum (FBS, Gibco, USA) and 1% penicillin/streptomycin (Sigma-Aldrich, St. Louis, MO) at 37°C in 5% CO$_2$. The fourth to sixth passage cells were used for the following experiments.

Bioactivities of OGP and BMP-2 released were assessed by measuring the effects of the release media on the proliferation and differentiation of BMSCs. Cell responses (PMs, PMs [OGP/BMP-2], PMs [OGP], and PMs [BMP-2]) were tested by an indirect method adapted from ISO 10993:5, 10993:12 and Fischer et al.[22] BMSCs were plated in a 24-well plate (0.5 $\times$ 10^4 cells/well), and 1.5 mL of normal

medium (DMEM supplemented with 10% FBS and 1% penicillin/streptomycin) was added. After culture for 24 h to allow cell attachment, the four types of microspheres were added separately to the wells (2 mg/well) and the plate was cultured with one change of media every 2 days. Cell culture without microspheres were used as the blank control.

After culture for 3–14 days, cell proliferation was evaluated by Alamar Blue assay. The optical density of the medium was measured at 570 and 600 nm (Moder MQX200, Bio Tek, GA). Cell morphology was studied by fluorescence and immunofluorescence staining. First, after culture for 7 days, living cells were stained with calcein-AM and their nuclei were stained with Hoechst 33258 (both Sigma). After rinse two times with PBS, thee parallel samples per group were observed under a fluorescence microscope (Olympus BX53). Additionally, for preparing positive control of cell differentiation, culture medium was replaced with an osteogenic-inducing medium (normal medium supplemented with 10 mM b-glycerol phosphate, 0.1 μM dexamethasone, and 50 μg/mL L-ascorbic acid (all Sigma)). After culture for 14 days, cells were fixed with 2.5% glutaraldehyde in PBS for 15 min. The samples were washed with PBS after each subsequent step at room temperature. Actin microfilaments were identified with TRITC-conjugated phalloidin (Sigma); osteocalcin (OCN) was identified with anti-OCN antibody and FITC-labeled goat-anti-rabbit IgG (Abcam, Cambridge, MA); and nuclei stained with 4',6-diamidino-2-phenylindole (DAPI, Sigma). Cell cytoskeleton arrangement and OCN distribution were observed with the fluorescence microscope. Parameters of the cells were analyzed statistically by image analyses of five micrographs (Image J, Bethesda, MD). The alkaline phosphatase (ALP) activity was measured with an ALP assay kit (Jiancheng Biotech, Nanjing, Jiangsu, China). After culture for 14, 21, and 28 days, the medium was discarded and the cells rinsed twice with PBS. Then, 1 mL of 1% Triton X-100 (w/v, Sigma) was added to lyse the cells, and the total protein concentration in the lysate was measured with BCA kits (Jiancheng Biotech). The final ALP activity of each well was normalized against the total protein content measured from the corresponding lysate. Similarly, after the addition of microspheres, BMSCs were cultured in osteogenic-inducing medium for 28 days and then fixed with 2.5% glutaraldehyde in PBS for 4 h at 4°C. The fixed cells were washed with distilled water to remove any salt residues before they were covered in 2% Alizarin Red S (ARS, pH 4.2) for 30 min at room temperature. Finally, the stained cells were rinsed several times with distilled water and then imaged by light microscope.

Statistical analysis
Data were analyzed by one-way analysis of variance (ANOVA) and subsequent Tukey multiple-comparison test. A p values < 0.05 was considered statistically significant.

RESULT
Formation of porous PLGA microspheres
By introducing NH_4HCO_3 as a gas foaming agent in W_1 (Supporting Information Fig. S2), porous PLGA microspheres (Fig. 2A) were formed. When the primary emulsion W_1/O has been added to W_2 and the oil phase was being evaporated off, NH_4HCO_3 in W_1 hydrolyzed to generated gas bubbles (i.e., CO_2 and NH_3), creating open pores in the microspheres. The effect of NH_4HCO_3 concentration was examined, and it was found that with increasing NH_4HCO_3 (0–20 mg in W_1) the microspheres (Fig. 2A) changed from a nonporous structure to an open-cellular structure. Their mean diameters (Fig. 2B) increased from 35.0 ± 15.5 to 149.0 ± 25.5 μm, and the pore sizes (Fig. 2B) enlarged from 0 to 17.5 ± 5.5 μm. The increasing microsphere size was attributable to the increased gas formation in W_1, which expanded the oil phase gas to produce larger microspheres. Likewise, the enlarged pore size was explained by the increased volume ratio between the gas formed and the oil phase. Five milligrams of NH_4HCO_3 was selected as the optimum porogen level; at this porogen dose, the interconnected pores were induced and uniformly distributed in the obtained microspheres with the mean microsphere diameter of 108 ± 20.5 μm and the mean pore diameter of 6 ± 2.5 μm.

Pore-closing treatment
OGP was loaded in the porous PLGA microspheres by soaking. To retard OGP release from the microspheres, the pores on their surfaces were closed by treatment with an aqueous AN solution (3–10%, v/v). After treatment, the pores diameter (Fig. 2C) gradually shrank with increasing AN concentration (3% AN: 4.5 ± 0.6 μm, 10% AN: 0.4 ± 0.1 μm; Fig. 2D). Interestingly, the microsphere diameter (Fig. 2C) was also reduced after this treatment (3% AN: 78 ± 8.5 μm, 10% AN: 36 ± 12.5 μm; Fig. 2D). This treatment was based on the different dissolving properties of PLGA in AN and water. AN is an effective solvent for PLGA whereas water is a nonsolvent. Consequently, aqueous AN solutions allowed relaxation movement of PLGA chains without dissolving the polymer. Driven by thermodynamics to reduce the specific surface area (i.e., surface energy), the chain movement led to gradual collapse of the pores, forming a barrier against OGP release. The optimum AN concentration was selected as 10%, because this level was effective at closing pores, and if higher than this level, microspheres would undergo collision-induced fusion and gradually lost the spherical geometry.

Surface modification of microspheres by PEI immobilization
The PLGA used in this study had an uncapped free —COOH group at one terminus, which was expected to be preferentially oriented toward the aqueous phase when porous PLGA microspheres were hydrated.[18] The exposed —COOH groups were conjugated with PEI via EDC/NHS chemistry to produce surface amine groups.[23–25] PEI is widely used as a precursor molecule enabling LbL assembly[26,27] because of its abundant —NH_2 groups ensuring more binding sites for the next polyelectrolyte layer.[28] PEI can be cytotoxic depending on the concentration, charge density, and molecular weight.[29,30] It was reported that, PEI <2000 Da had no cytotoxic effect.[29] In the present study, a 600 Da PEI was
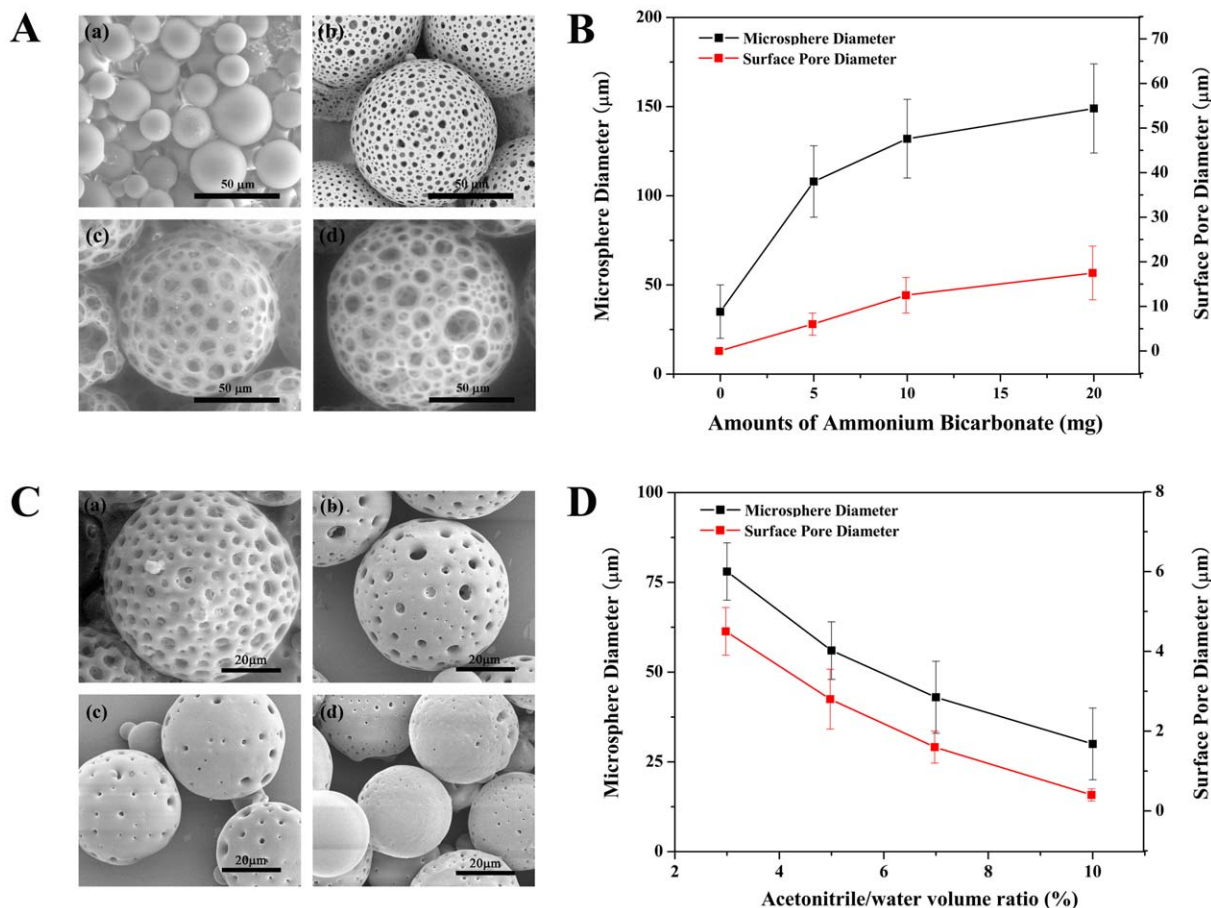
FIGURE 2. Morphology of microspheres was prepared at various conditions. Left column: scanning electron microscopy; right column: average diameter of microspheres. Conditions were controlled (A, B) by varying the amounts of ammonium bicarbonate in the W_1 phase: (a) 0 mg; (b) 5 mg; (c) 10 mg; and (d) 20 mg, (C, D) by varying acetonitrile concentrations for pore-closing process: (a) 3%; (b) 5%; (c) 7%; and (d) 10%.

used to modify PLGA microspheres. SEM (Fig. 3A(a)) found that, after PEI immobilization, microspheres retained their spherical morphology. After FITC labeling, green fluorescence can be detected at the entire surface of microsphere by confocal fluorescence microscopy (Supporting Information Fig. S3), confirming the uniform distribution of PEI molecules immobilized on their surfaces.

Layer-by-layer coating of biopolyelectrolytes on microspheres

Polyelectrolytes (i.e., HA, CS) were LbL deposited on PEI-immobilized microspheres via EDC/NHS coupling between the amino groups (CS) and carboxyl groups (HA and Hep). Because of the fact that the N-terminal region of BMP-2 has binding sites for Hep,[31] a BMP-2 layer was inserted between two Hep layers, thus becoming loaded onto microspheres. In our design, the addition of Hep could facilitate the binding of BMP-2 to the polyelectrolyte layers so as to increase BMP-2 loading. To account for the higher surface-area-to-volume ratio in the microsphere system, we also deposited two bilayers of HA-CS to ensure uniform coverage before deposition of Hep and BMP-2. In fact, it has been reported

that this method of coupling proteins by LbL assembly can not only effectively decrease the diffusion of factors through layers, but also prolong their half-life and maintain their bioactivity.[19,32]

The LbL coating was verified by confocal microscopy after labeling CS with Rhodamine-B (second layer) and FITC (eighth layer). Labeled microspheres (Fig. 3B) emitted red and green fluorescent signals, indicating the formation of a complete LbL coating. The signals were somewhat nonuniform, which may be related to the partially closed micropores on the microsphere surface. SEM found that no noticeable difference in particle size or geometry before and after LbL coating (Fig. 3A).

Physicochemical characteristics of layer-by-layer coated microspheres

Compared with unmodified PLGA microspheres (Fig. 3C), PLGA-PEI gave two additional sharp peaks at 1640, 1537 cm^{-1} (amide I and II stretching) and a broad peak at 3350–3500 cm^{-1} (—NH$_2$ stretching of PEI) while the —NH$_2$ bending peaks of PEI (1590–1650 cm^{-1}) were weaken, confirming PEI linkage to PLGA via amide bonds. In the spectrum of
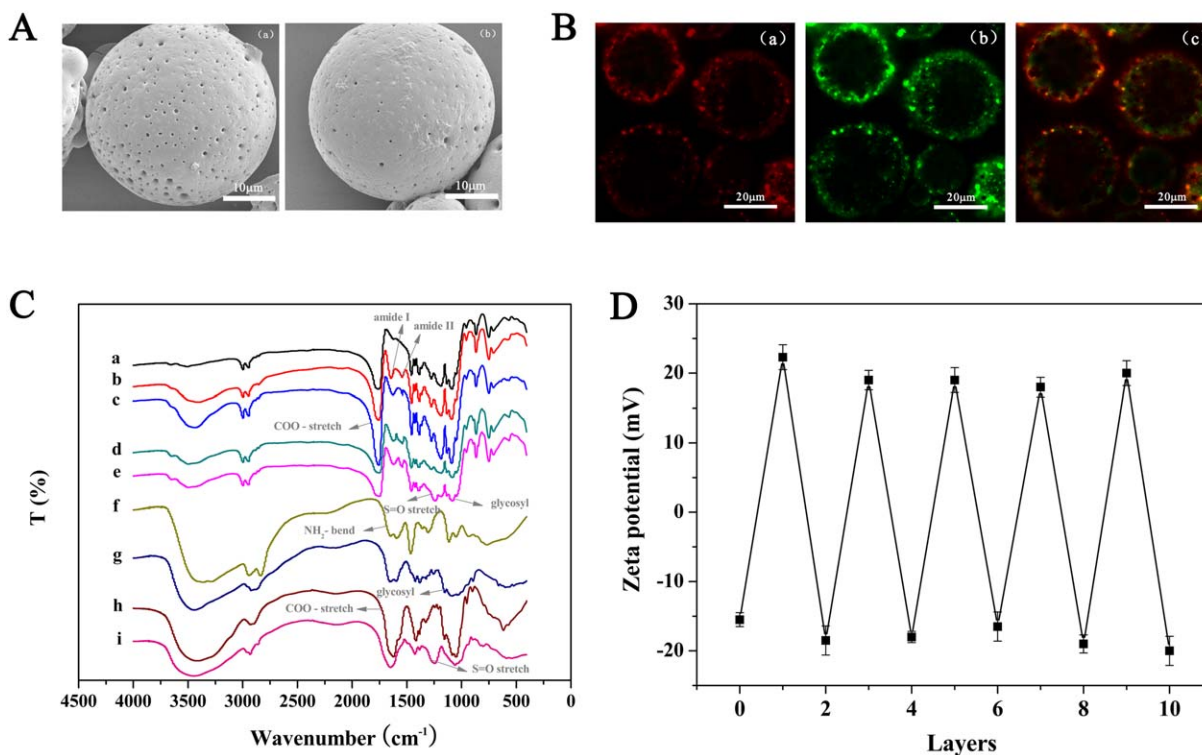
FIGURE 3. Characterization of the multilayered microspheres: (A) scanning electron microscopy images of (a) PEI-immobilized PLGA microspheres and (b) layer-by-layer coated PLGA microspheres. B: Confocal scanning light microscopy image of PLGA microspheres coated with a layer-by-layer assembly of (HA-CS)$_4$ including (a) Rhodamine-B-labeled CS which appears red and (b) FITC-labeled CS which appears green, in the second and the eighth layers, respectively. Both fluorophores appear in the overlay image (c). C: ATR FTIR spectra of PLGA surfaces treated with variety of biological molecules: (a) PLGA, (b) PLGA-PEI, (c) PLGA-PEI-HA, (d) PLGA-PEI-HA-CS, (e) PLGA-PEI-HA-CS-Hep, (f) PEI, (g) CS, (h) HA, and (i) Hep. D: Zeta potential surface charge alternation with the adsorption of each polyelectrolyte layer.

PLGA-PEI-HA, the peak at 1755 cm^{-1} (C═O stretching of —COOH) became slightly stronger (vs. PLGA-PEI), consistent with the deposition of an HA layer. In PLGA-PEI-CS, a wide band appeared at ~1100 cm^{-1}, corresponding to the stretching of glucosyl structure in CS. In PLGA-PEI-CS-Hep, a new peak appeared at 1244 cm^{-1} (asymmetric stretching of SO$_2^-$), consistent with Hep deposition. Similarly, the other spectra showed patterns consistent with LbL coating.

The unmodified PLGA microspheres had a positive Zeta potential (~15 mV). After PEI immobilization, it switched to 22.3 ± 1.8 mV. During subsequent LbL coating, the Zeta potential cycled regularly between negative (~−19 mV) and positive (~+19 mV) values (Fig. 3D), as expected from the alternating deposition of —NH$_2$ and —COOH groups on the microspheres.

Biofactor release

ELISA found that, after solution soaking, the unmodified porous microspheres encapsulated 396 ng of OGP per 1 mg of microspheres, with an encapsulation efficiency of 39.6%. The microspheres released 68.4% of the loaded OGP within 3 days (Fig. 4, blue line). This fast release is explained by the free diffusion of OGP molecules via pores and interconnected channels in the microspheres without physical barriers.

In comparison, the LbL-coated microspheres carried 209 ng of OGP and 110 ng of BMP-2 per 1 mg of microspheres,

corresponding to encapsulation efficiencies of 20.9% and 14.7%, respectively. They gradually released <17.1% of the loaded OGP and 60.3% of BMP-2 in 15 days. At 60 days, they released 96.4% of the BMP-2 (Fig. 4, red line and black line). Their slow release patterns were attributed to the closure of surface pores (for OGP) and creation of a diffusion barrier (i.e., LbL coating; for OGP and BMP-2). After pore closing, OGP released from microspheres might occur mainly via diffusion through the junction gaps of the collapsed pores. After LbL coating, the deposited Hep, CS, and HA capping layers on the microspheres provided a tortuous path for biofactor diffusion. Hence, BMP-2 was released in a gradual and sustained manner. We suspect that this may be the result of a slow dissociation of the biomolecule layers. In addition, by comparing the results of ELISA analysis with those of BCA analysis, it was found that the cumulative release amount and the total loading amount of BMP-2 measured by ELISA and BCA assay respectively were nearly equal, indicating that all of BMP loaded on the microspheres could effectively bind antibodies in the enzyme-linked immunosorbent response, which further demonstrated that the conformation of BMP-2 had not changed. Besides, 80.3% of the OGP initial input amount in the scaffolds was detected in the release medium after 60 days by ELISA assay, suggesting most of the OGP remained the structural integrity and original conformation.[33]
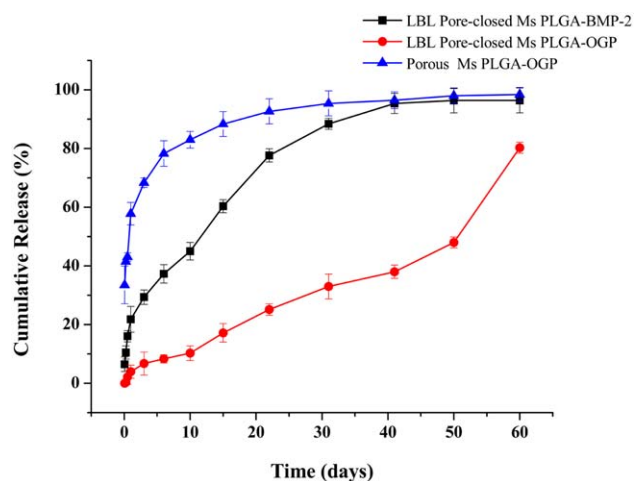
FIGURE 4. Release of OGP and BMP-2 from layer-by-layer coated PLGA microspheres as assessed by ELISA. The cumulative mass of OGP and BMP-2 released is expressed as a percentage of the mass of OGP and BMP-2 loaded onto the PLGA microspheres. Each data point is the mean of three replicates ($n = 3 \pm$ s.e.m.).

Bioactivity of OGP and BMP-2 released from layer-by-layer coated microspheres

Cell morphology. After culture for 7 days, cytoplasm and nuclei of BMSCs were stained, and observed by fluorescence microscopy. Generally, the BMP-2 and OGP released from all of the PLGA microsphere groups stimulated the growth of BMSCs *in vitro*, confirming that the biofactors remained bioactive and the microspheres were biocompatible. The cells (Fig. 5A) were viable and adhered to all samples, but the differences were observed in cell density and morphology. Relatively more BMSCs adhered on PMs and PMs (OGP), showing a more rounded cytoskeleton development. In comparison, those cultured on PMs (OGP/BMP-2) and PMs (BMP-2) became more elongated and formed longer thin pseudopodia.

Cell proliferation. Quantitative assays (Fig. 5B) found that, BMSCs seeded on all samples increased in number during culture, as same as the blank control group, indicating that all samples were safe and supported cell proliferation. After 7 days, the proliferation of BMSCs on PMs and PMs (OGP) were slightly higher compared with those seeded on microspheres carrying BMP-2. This hinted that BMP-2 may have promoted the differentiation of BMSCs (see below), leading to a slower proliferation. However, after 14 days, the cell number was the highest on the microspheres simultaneously carrying OGP and BMP-2. It was supposed that although the early release of BMP-2 slowed BMSCs proliferation, the later release of OGP could stimulate the growth of preosteoblast which were induced to form by BMP-2. These findings indicated that, OGP and BMP-2 synergistically worked to promote cell proliferation.

Meanwhile, cell proliferation rates on PMs and PMs (OGP) were nearly equal at all three time points (Fig. 5B). This showed that, in the absence of BMP-2 (an osteogenic inductor), OGP released alone did not noticeable affect BMSCs proliferation. This was consistent with what was observed under fluorescence microscopy (Fig. 5A).

Cell differentiation. ALP level was used as an indicator for BMSCs differentiation. After culture for 14, 21, and 28 days, the cells seeded on PMs (OGP/BMP-2) (Fig. 5C) consistently had significantly higher ALP levels than those of other groups (all $p < 0.05$). This result indicated that OGP and BMP-2 also functioned synergistically on BMSCs differentiation.

Based on the release curves (Fig. 4), we suggest that, the initial OGP released for 14 days was so low that BMP-2 played a key role in increasing the ALP level in the cells. Hence, the ALP activities in BMSCs seeded on the microspheres containing BMP-2 alone and those simultaneously containing two biofactors were higher than those seeded on the microspheres carrying OGP alone. After culture for 21 days, ALP activity increased on all substrates, demonstrating that all samples supported cell differentiation. It is worth noting that there were no significant differences between the cells seeded on PMs (OGP) and the cells seeded on PMs (BMP-2). This may be due to the fact that, after 21 days, OGP release was accelerated to stimulate the proliferation of osteoblasts and strikingly enhance the ALP activity. However, the ALP levels recorded from all groups decreased after culture for 28 days, in contrast to cultivation for 21 days, and this downward trend was more obvious in the cells seeded on PMs (OGP) and those seeded on PMs (OGP/ BMP-2) than in other groups. These changes may be explained by the facts that further calcium deposits inhibited ALP expression and OGP also could significantly stimulate the cell calcification.[34]

The mineralized matrix synthesis was assessed using an ARS staining assay, which identified calcium deposition. After differentiation for 28 days, the calcium deposition was stained with red spots (Fig. 5D) The color intensity of the PMs (BMP-2/OGP) and PMs (OGP) groups was obviously stronger than the others, especially the PMs (BMP-2/OGP) group, which supported the previously described results regarding the ALP activity measurement.

Immunostaining. Immunofluorescence staining of cytoskeletal actin (Fig. 6A) revealed that the cells seeded on PMs (BMP-2) and those seeded on PMs (OGP/BMP-2) developed a parallel, unidirectional organization of the actin cytoskeleton and a remarkable stretching, as opposed to the multidirectional actin cytoskeleton in other groups. Therefore, the cell elongation and adhesion appeared to be related to the BMP-2 released. To quantify the differences in cell morphology observed in the immunofluorescence images, the major and minor axes were measured and the major/minor ratio was used as the elongation ratio. It was found that (Fig. 6B), the cells seeded on PMs (BMP-2) and those seeded on PMs (OGP/BMP-2) had the mean cell elongation ratios of 4.2–6.5, whereas those seeded on PMs exhibited a mean elongation ratio of nearly 1 (i.e., isotropic shape).

Interestingly, the nuclei of cells (Fig. 6C) seeded on PMs (BMP-2) and those seeded on PMs (OGP/BMP-2) were also observed to have a similar trend of increased elongation,
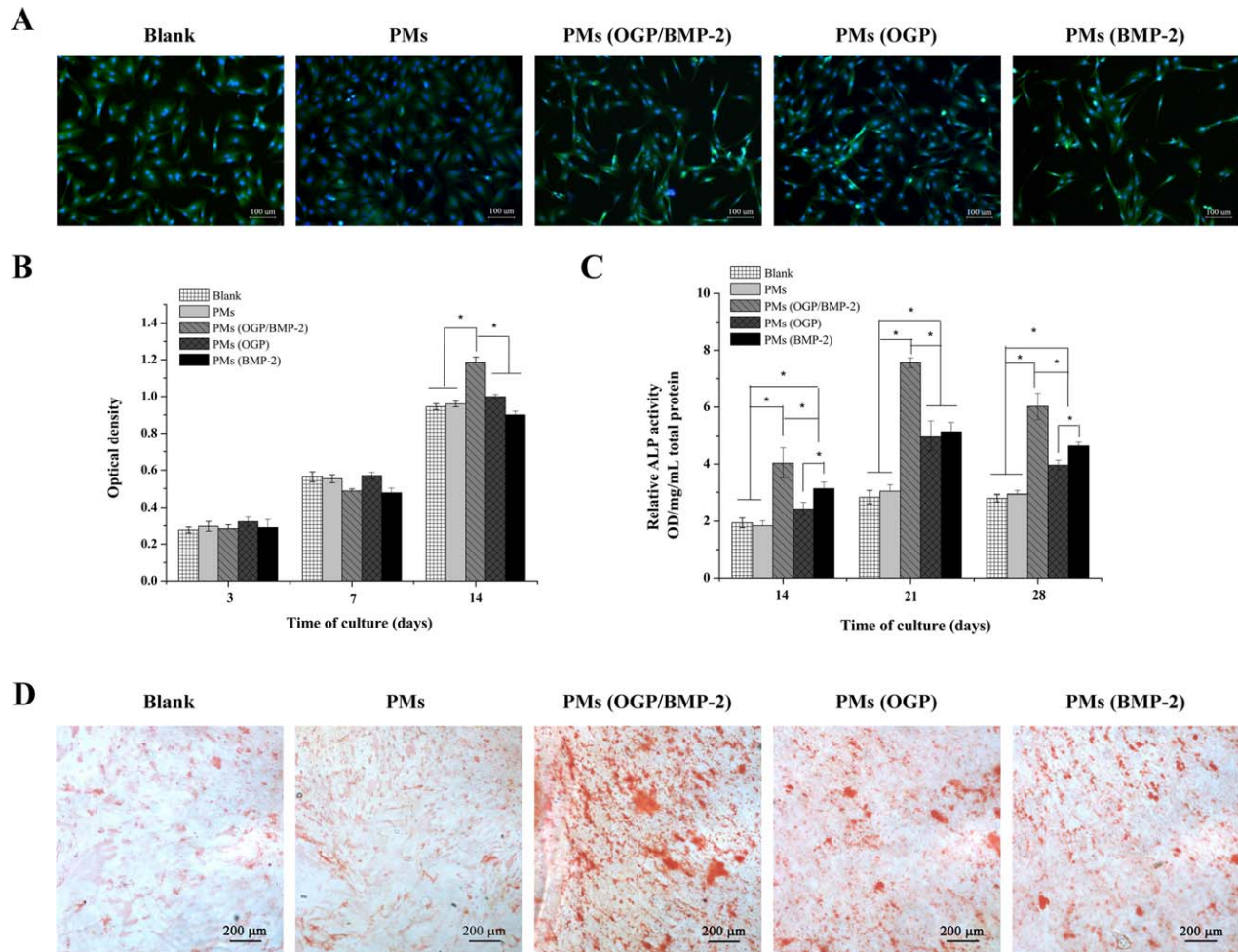
FIGURE 5. Cell adhesion, proliferation and differentiation on various microspheres. A: Spread and cytoskeletal arrangement of BMSCs incubated with PMs, PMs (OGP/BMP-2), PMs (OGP), and PMs (BMP-2) microspheres for 7 days. Representative fluorescent images with dual staining Hoechst 33258 for nuclei (blue) and calcein-AM for cytoplasm (green) are shown. B: Cell proliferation of BMSCs on various substrates after 3, 7, and 14 days of incubation. C: ALP activity of BMSCs cultured on different substrates for 14, 21, and 28 days. D: Osteogenic differentiation of BMSCs measured by Alizarin Red staining at 28 days. Results are the mean $\pm$ standard deviation ($n = 4$). Asterisk (*) indicates the significant difference ($p < 0.05$).

with the latter group being most evident. The shape index, or circularity of cell nuclei defined as $4\pi \times$ area/perimeter^2, was used to quantify nuclear deformation, with a score of 1 representing a perfect circle while values far <1 correspond to high-aspect-ratio geometries.[35] The cells seeded on the factor-free microspheres (Fig. 6C) exhibited a shape index of 0.91, compared with 0.82, 0.85, and 0.80 in those seeded on PMs (OGP), PMs (BMP-2), and PMs (OGP/BMP-2), respectively. We speculated that, the nuclear organelle elongation on the factor(s)-loaded microspheres was partly due to the elongated cytoskeletal morphology of the cells. The increased elongation/stretching of cell bodies on PMs (BMP-2) and PMs (OGP/BMP-2) probably led to a preferential differentiation into the osteogenic lineage, which was confirmed by immunofluorescent staining of OCN (Fig. 6A).

Fluorescence microscopy (Fig. 6A) found that the OCN signal intensity was weak in the cells seeded on PMs and cells on PMs (OGP), indicating limited OCN in their cytoplasms. In comparison, the cells seeded on PMs (BMP-2)

and, particularly, those on PMs (OGP/BMP-2) produced substantially stronger signals, coinciding with the previous conclusions obtained from the results of staining of cytoskeletal actin. It has been reported that cell morphology is closely related to cell function and the change of nuclear shape can promote the expression of differentiation genes. Kumar et al.[36] studied the association between the geometry and differentiation of BMSCs cultured on biomaterial surfaces and found that the length/width ratio of cells that had differentiated into the osteogenic direction was significantly higher than those toward adipogenic differentiation. Brammer et al. also observed that the ability of cells to differentiate into osteoblasts increased with the aspect ratio,[37,38] consistent with to our findings.

Therefore, these results showed that the layer-by-layer coated pore-closed PLGA microspheres developed in this study effectively realized the sequential release of BMP-2 and OGP, and their release effectively produced synergistic biological effects on BMSCs in vitro. The approach reported
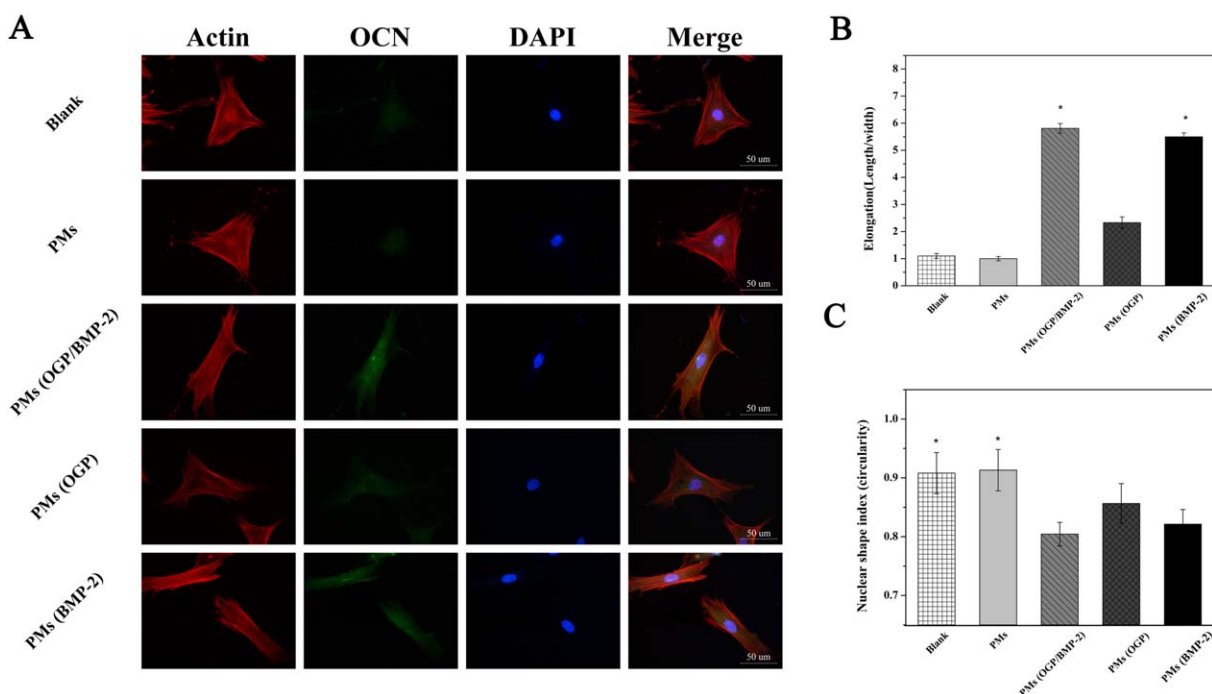
FIGURE 6. Cell morphology observed in the immunofluorescence images and cell osteogenic differentiation related protein expression on various microspheres. A: Immunofluorescence analysis of OCN expression (green) in BMSCs cultured with PMs, PMs (OGP/BMP-2), PMs (OGP), and PMs (BMP-2) microspheres. Nuclei were stained by DAPI (blue) and cytoskeleton filaments were stained by TRITC-phalloidin (red). B: Cell elongation ratio and (C) nuclear shape index or circularity at 14 days, calculated from the images in (A). Results are the mean ± standard deviation ($n = 4$). Asterisk (*) indicates the significant difference ($p < 0.05$).

here may be useful for releasing two biofactors to address different stages of bone healing.

DISCUSSION

Biomaterials-based controlled release strategies have been studied widely and applied in tissue engineering. In modern design, a multiple drug delivery system with a sequential release profile is considered to be able to effectively repair and regenerate tissues including bone. Raiche and Puleo proposed an approach utilizing a bilayered gelatin coating to incorporate insulin-like growth factor-1 (IGF-1) and BMP-2 together. The coating was able to deliver two loaded GFs in a controlled sequential manner within 2 weeks.[39] Although a sequential release could be achieved by this approach, the protein instability and rapid release of biofactors made it unable to meet the requirement of bone repair, which usually requires months. Recently, Wang et al.[3] reported core–shell microspheres simultaneously incorporating angiogenic and osteogenic factors. In their study, FGF-2 was incorporated in a PLGA-based shell and BMP-2 in a PLLA-based core. The two GFs could be released from the two matrices at significantly different rates over several weeks to months, showing a possible synergistic role of FGF-2 with BMP-2 in the bone regeneration process. However, this technique may not be suitable for other bioactive molecules, because it uses organic solvents to dissolve polymer matrices, oil–water interfaces and surfactants, which may adversely affect the bioactivity of the cargo molecules.

In this study, the multilayered pore-closed PLGA microsphere was used as a multibarrier carrier for BMP-2 and OGP delivery, and was confirmed to be an effective way to achieve a long-term sustained release of biofactors and maintain their bioactivity. Notably, the pore-closing-LbL coating approach not only delayed OGP release but also produced a sequential release. The OGP release was minimal in the first 20 days but accelerated remarkably thereafter. Comparatively, the BMP-2 release was predominant in the first 20 days and only marginal subsequently (Fig. 4). These contrasting behaviors demonstrated that this approach could produce a sequential release of two biofactors for targeting different bone healing stages. It will be interesting to investigate the possibility of sequential release of even more biofactors through further development of the carrier microstructures.

BMP-2 is well known as a strong inducer of bone formation,[40] which has been demonstrated to potently induce the differentiation of a variety of cell types into osteoblast precursors.[41] Interestingly, it was observed that the proliferative roles of proliferative agents (FGF-2) were interfered by BMP-2 when they existed together in cell culture. BMP-2-induced inhibition of cell proliferation may be attributed to the fact that BMP-2 may have signaled some MSCs to differentiate toward the osteogenic lineage and, accordingly, may have lost their proliferation ability.[42] Other studies reported that OGP could effectively accelerate osteocyte proliferation, regulate ALP activity, and enhance OCN secretion and matrix

mineralization via an auto-regulated feedback mechanism.[34] Accordingly, OGP effectively promoted the density of newly formed bones and stimulates bone healing.[43,44] In view of the unique biological effects of the two biofactors and their sequential release from PLGA microspheres, this carrier model is expected to regulate the primary and secondary roles of OGP and BMP-2 at the different stages of osteogenesis, showing induction-oriented function by BMP-2 in the early stage while mainly modulation by OGP in the late. To test this hypothesis, cell proliferation, cell morphology and ALP activities, calcium deposition as well as OCN protein secretion of BMSCs were assessed. In our experiment, *in vitro* cell culture demonstrated that the cell proliferation on the OGP/BMP-2-loaded microspheres were lower than those observed in the other groups in the first 7 days, but increased to become the highest of all groups on day 14 (Fig. 5B). This difference can be ascribed to the synergistic effect of these biofactors coencapsulated in the same microsphere with distinct release profiles. In other words, OGP could modulate the effect of BMP-2 on stem cell differentiation, which was evidenced by the fact that the first release of BMP-2 induced the transformation of BMSCs into osteoblasts and then the followed release of OGP stimulated osteoblast precursors activity, enhanced cell proliferation and improved ossification. The *in vitro* osteogenesis study showed that the ALP activity in the PMs (OGP/BMP-2) group was elevated at all-time points compared with those in other groups (Fig. 5C), suggesting that the sustained sequential release of BMP-2 and OGP could continually and synergistically stimulate ALP expression. In fact, previous studies have confirmed that in the repair of bone defects or fractures, a simple combination of two or more GFs that take different roles or are active during different stages of natural bone repair is advantageous over single GF in most cases.[45,46] Therefore, the couse of OGP and BMP-2 is considered a rational strategy to stimulate osteogenesis *in vitro* for subsequent bone tissue engineering. Our *in vitro* characterization of OCN protein immunostaining at 14 days revealed that the effects of OGP on BMSCs behavior and cell morphology were substantially weaker compared with the synergistic involvement of OGP and BMP-2 (Fig. 6). At the same time, these biological effects also indicated that the BMP-2 and OGP released from multilayered microspheres did not lose significant bioactivity after encapsulation. In summary, the layer-by-layer coated pore-closed PLGA microspheres developed in the current study achieved a sequential release of two biofactors, providing an interesting possibility for the repair of bone defects.

CONCLUSIONS

In the present study, dual-biofactor-loaded multilayered PLGA microspheres were fabricated and characterized. *In vitro* release experiments revealed that the pore-closing process and multilayer assembly of polyelectrolytes on a microsphere system not only provided sustained delivery of biologically relevant levels of OGP and BMP-2 but also regulated the sequential release of two biofactors. The release patterns effectively made the encapsulated proteins synergistically exert their biological activity in *in vitro* cell experiments. In summary, these results indicated that the prepared microspheres not only facilitated cell proliferation, but also contributed to cell differentiation. The sequential dual-biofactor-controlled release led to an increase in elongation/stretching of cell bodies, upregulation of bone-related protein expression and even a greater bone-forming ability. The current delivery strategy will have great potential for sustained release of various hydrophilic macromolecules including peptides, proteins and DNA to create a range of tailored multilayered microspheres. Based on these results, we expect that multilayered microspheres can be combined with tissue engineering scaffolds for drug delivery. In future research, we will optimize this system by minimizing drug loss during processing to improve the loading efficiency and investigate their distribution on 3D porous scaffolds to evaluate their potential in the bone reconstruction.

REFERENCES

1. Browne S, Pandit A. Multi-modal delivery of therapeutics using biomaterial scaffolds. J Mater Chem B 2014;2:6692–6707.
2. Kim YH, Tabata Y. Dual-controlled release system of drugs for bone regeneration. Adv Drug Deliv Rev 2015;94:28–40.
3. Wang S, Ju W, Shang P, Lei L, Nie HM. Core–shell microspheres delivering FGF-2 and BMP-2 in different release patterns for bone regeneration. J Mater Chem B 2015;3:1907–1920.
4. Shen XF, Zhang YX, Gu Y, Xu Y, Liu Y, Li B. Sequential and sustained release of SDF-1 and BMP-2 from silk fibroin-nanohydroxyapatite scaffold for the enhancement of bone regeneration. Biomaterials 2016;106:205–216.
5. Volpato FZ, Almodóvar J, Erickson K, Popat KC, Migliaresi C, Kipper MJ. Preservation of FGF-2 bioactivity using heparin-based nanoparticles, and their delivery from electrospun chitosan fibers. Acta Biomater 2012;8:1551–1559.
6. Saltzman WM, Olbricht WL. Building drug delivery into tissue engineering design. Nat Rev Drug Discov 2002;1:177–186.
7. Perez RA, Kim JH, Buitrago JO, Wall IB, Kim HW. Novel therapeutic core–shell hydrogel scaffolds with sequential delivery of cobalt and bone morphogenetic protein-2 for synergistic bone regeneration. Acta Biomater 2015;23:295–308.
8. Makadia HK, Siegel SJ. Poly lactic-*co*-glycolic acid (PLGA) as biodegradable controlled drug delivery carrier. Polymers 2011;3: 1377–1397.
9. Kim HK, Park TG. Microencapsulation of human growth hormone within biodegradable polyester microspheres: Protein aggregation stability and incomplete release mechanism. Biotechnol Bioeng 1999;65:659–667.
10. Sah H. Protein instability toward organic solvent/water emulsification: Implications for protein microencapsulation into microspheres. J Pharm Sci Technol 1999;53:3–10.
11. Sun L, Zhou SB, Wang WJ, Li XH, Wang JX, Weng J. Preparation and characterization of porous biodegradable microspheres used for controlled protein delivery. Colloids Surf A Physicochem Eng Asp 2009;345:173–181.
12. Lee J, Oh YJ, Lee SK, Lee KY. Facile control of porous structures of polymer microspheres using an osmotic agent for pulmonary delivery. J Control Release 2010;146:61–67.
13. Hong GY, Jeong YI, Lee SJ, Lee E, Oh JS, Lee HC. Combination of paclitaxel- and retinoic acid-incorporated nanoparticles for the treatment of CT-26 colon carcinoma. Arch Pharm Res 2011;34: 407–417.
14. Ganta S, Amiji M. Coadministration of paclitaxel and curcumin in nanoemulsion formulations to overcome multidrug resistance in tumor cells. Mol Pharm 2009;6:928–939.
15. Park JS, Yang HN, Jeon SY, Woo DG, Na K, Park KH. Osteogenic differentiation of human mesenchymal stem cells using RGD-

modified BMP-2 coated microspheres. Biomaterials 2010;31:6239–6248.

16. Park JS, Park K, Woo DG, Yang HN, Chung HM, Park KH. Triple constructs consisting of nanoparticles and microspheres for bone-marrow-derived stromal-cell-delivery microscaffolds. Small 2008;4:1950–1955.

17. Narayanan S, Pavithran M, Viswanath A, Narayanan D, Mohan CC, Manzoor K, Menon D. Sequentially releasing dual-drug-loaded PLGA–casein core/shell nanomedicine: Design, synthesis, biocompatibility and pharmacokinetics. Acta Biomater 2014;10:2112–2124.

18. Chung HJ, Kim HK, Yoon JJ, Park TG. Heparin immobilized porous PLGA microspheres for angiogenic growth factor delivery. Pharm Res 2006;23:1835–1841.

19. Go DP, Palmer JA, Mitchell GM, Gras SL, O'Connor AJ. Porous PLGA microspheres tailored for dual delivery of biomolecules via layer-by-layer assembly. J Biomed Mater Res A 2015;103A:1849–1863.

20. Westall FC, Rubin R, Gospodarowicz D. Brain-derived fibroblast growth factor: A study of its inactivation. Life Sci 1983;33:2425–2429.

21. Kyobum K, David D, Antonios GM, John PF. Effect of initial cell seeding density on early osteogenic signal expression of rat bone marrow stromal cells cultured on cross-linked poly(propylene fumarate) disks. Biomacromolecules 2009;10:1810–1817.

22. Fischer J, Profrock D, Hort N, Willumeit R, Feyerabend F. Reprint of: Improved cytotoxicity testing of magnesium materials. Mater Sci Eng B 2011;176:1773–1777.

23. Hermanson GT. Bioconjugate Techniques. Vol. 746. San Diego, CA: Academic Press; 1996. p 673–725.

24. Yoon JJ, Song SH, Lee DS, Park TG. Immobilization of cell adhesive RGD peptide onto the surface of highly porous biodegradable polymer scaffolds fabricated by a gas foaming/salt leaching method. Biomaterials 2004;25:5613–5620.

25. Jeon O, Kang SW, Lim HW, Chung JH, Kim BS. Long-term and zero-order release of basic fibroblast growth factor from heparin-conjugated poly(l-lactide-co-glycolide) nanospheres and fibrin gel. Biomaterials 2006;27:1598–1607.

26. Croll TI, O'Connor AJ, Stevens GW, Cooper-White JJ. A blank slate layer-by-layer deposition of hyaluronic acid and chitosan onto various surfaces. Biomacromolecules 2006;7:1610–1622.

27. Facca S, Cortez C, Mendoza-Palomares C, Messadeq N, Dierich A, Johnston APR, Mainard D, Voegel JC, Caruso F, Benkirane-Jessel N. Active multilayered capsules for in vivo bone formation. Proc Natl Acad Sci USA 2010;107:3406–3411.

28. Croll TI, O'Connor AJ, Stevens GW, Cooper-White JJ. Controllable surface modification of poly(lactic-co-glycolic acid) (PLGA) by hydrolysis or aminolysis I: Physical, chemical, and theoretical aspects. Biomacromolecules 2004;5:463–473.

29. Yang YW, Hsu PYJ. The effect of poly(D,L-lactide-co-glycolide) microparticles with polyelectrolyte self-assembled multilayer surfaces on the cross-presentation of exogenous antigens. Biomaterials 2008;29:2516–2526.

30. Beyerle A, Hobel S, Czubayko F, Schulz H, Kissel T, Aigner A, Stoeger T. In vitro cytotoxic and immunomodulatory profiling of low molecular weight polyethylenimines for pulmonary application. Toxicol In Vitro 2009;23:500–508.

31. Ruppert R, Hoffmann E, Sebald W. Human bone morphogenetic protein-2 contains a heparin-binding site which modifies its biological activity. Eur J Biochem 1996;237:295–302.

32. Zuo QH, Guo R, Liu Q, Hong A, Shi YF, Kong Q, Huang YX, He LM, Xue W. Heparin-conjugated alginate multilayered microspheres for controlled release of bFGF. Biomed Mater 2015;10:035008.

33. Vitalian B, Daniela G, Anna B, Camillo S. Monoclonal antibodies as a probe for the unfolding of porcine growth hormone. J Immunol Methods 2003;272:107–115.

34. Gabet Y, Müller R, Regev E, Sela J, Shteyer A, Salisbury K, Chorev M, Bab I. Osteogenic growth peptide modulates fracture callus structural and mechanical properties. Bone 2004;35:65–73.

35. Wang K, Cai L, Zhang L, Dong JY, Wang SF. Biodegradable photo-crosslinked polymer substrates with concentric microgrooves for regulating MC3T3-E1 cell behavior. Adv Healthcare Mater 2012;1:292–301.

36. Kumar G, Tison CK, Chatterjee K, Pine PS, McDaniel JH, Salit ML, Young MF, Simon CGS. The determination of stem cell fate by 3D scaffold structures through the control of cell shape. Biomaterials 2011;32:9188–9196.

37. Oh S, Brammer KS, Li YSJ, Teng D, Engler AJ, Chien S, Jin SH. Stem cell fate dictated solely by altered nanotube dimension. Proc Natl Acad Sci USA 2009;106:2130–2135.

38. Brammer KS, Oh SH, Cobb CJ, Bjursten LM, Heyde HVD, Jin SH. Improved bone-forming functionality on diameter-controlled $TiO_{(2)}$ nanotube surface. Acta Biomater 2009;5:3215–3223.

39. Raiche AT, Puleo DA. In vitro effects of combined and sequential delivery of two bone growth factors. Biomaterials 2004;25:677–685.

40. Chen D, Zhao M, Mundy GR. Bone morphogenetic proteins. Growth Factors 2004;22:233–241.

41. Marie PJ, Debiais F, Haÿ E. Regulation of human cranial osteoblast phenotype by FGF-2, FGFR-2 and BMP-2 signaling. Histol Histopathol 2002;17:877–885.

42. Zhu L, Skoultchi AI. Coordinating cell proliferation and differentiation. Curr Opin Genet Dev 2001;11:91–97.

43. Bab I, Chorev M. Osteogenic growth peptide: From concept to drug design. Biopolymers 2002;66:33–48.

44. Chen C, Li H, Kong XD, Zhang SM, Lee IS. Immobilizing osteogenic growth peptide with and without fibronectin on a titanium surface: Effects of loading methods on mesenchymal stem cell differentiation. Int J Nanomed 2015;10:283–295.

45. Kempen DH, Lu L, Heijink A, Hefferan TE, Creemers LB, Maran A, Yaszemski MJ, Dhert WJ. Effect of local sequential VEGF and BMP-2 delivery on ectopic and orthotopic bone regeneration. Biomaterials 2009;30:2816–2825.

46. Yilgor P, Hasirci N, Hasirci V. Sequential BMP-2/BMP-7 delivery from polyester nanocapsules. J Biomed Mater Res A 2010;93:528–536.